JACS
JOURNAL OF THE AMERICAN CHEMICAL SOCIETY

COMMUNICATION

pubs.acs.org/JACS

Encoding Complex Wettability Patterns in Chemically Functionalized 3D Photonic Crystals

Ian B. Burgess,*[,†] Lidiya Mishchenko,[†] Benjamin D. Hatton,[‡] Mathias Kolle,[†] Marko Lončar,[†] and Joanna Aizenberg*[,†,‡,§,∥]

[†]School of Engineering and Applied Sciences, [‡]Wyss Institute for Biologically Inspired Engineering, [§]Department of Chemistry and Chemical Biology, and [∥]Kavli Institute for Bionano Science & Technology, Harvard University, Cambridge, Massachusetts 02138, United States

Supporting Information

ABSTRACT: Much of modern technology—from data encryption to environmental sensors to templates for device fabrication—relies on encoding complex chemical information in a single material platform. Here we develop a technique for patterning multiple chemical functionalities throughout the inner surfaces of three-dimensional (3D) porous structures. Using a highly ordered 3D photonic crystal as a regionally functionalized porous carrier, we generate complex wettability patterns. Immersion of the sample in a particular fluid induces its localized infiltration and disappearance of the bright color in a unique spatial pattern dictated by the surface chemistry. We use this platform to illustrate multilevel message encryption, with selective decoding by specific solvents. Due to the highly symmetric geometry of inverse opal photonic crystals used as carriers, a remarkable selectivity of wetting is observed over a very broad range of fluids' surface tensions. These properties, combined with the easily detectable optical response, suggest that such a system could also find use as a colorimetric indicator for liquids based on wettability.

The ability to encode complex chemical information in a single system underlies much of modern technology, from encrypting messages and data,[1−3] to designing sensors that can distinguish among a wide range of stimuli,[4−6] to creating templates that direct the assembly or growth of materials.[7−12] Recently, spatially encoding of hydrophilicity has been used to manipulate the flow of water in three-dimensional (3D) porous networks,[13,14] a promising approach to simple and inexpensive fluidic and diagnostic devices. In this work we present a technique for chemical encryption in 3D porous photonic crystals, leading to many highly specific regioselective wetting patterns for different fluids. SiO_2 inverse opal films (IOFs) were chemically patterned via multiple iterations of alkylchlorosilane exposure and masked oxygen plasma exposure. When a thus-functionalized IOF is submerged in a solvent, only the regions having wettability above a specific threshold are expected to be infiltrated. Due to vastly different refractive-index contrast between the wetted and nonwetted regions, a visible pattern will be revealed. The ability to encode many different functionalities into a highly symmetric porous network will result in high density of chemical information and allow many different patterns to be revealed in different liquids with remarkable selectivity.

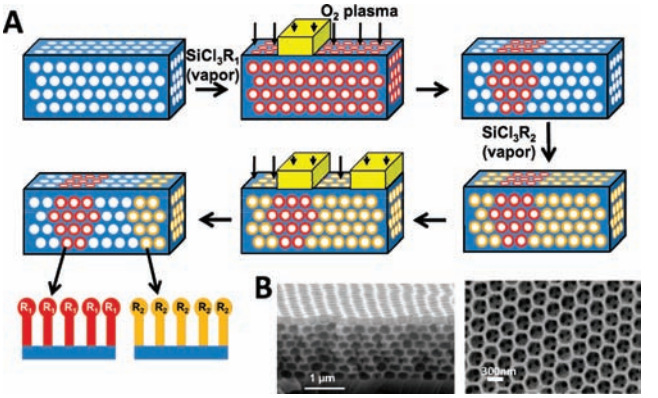

Figure 1. (A) Schematic of the chemical encoding procedure. The inner surfaces of IOFs are functionalized by repeated iterations of exposing the entire film to alkylchlorosilane vapors, followed by selective exposure to oxygen plasma, masked through slabs of PDMS, sealed on top of the film. (B) Scanning-electron micrographs of IOFs, left: cross section; right: top view.

The technique used to encode wettability patterns is outlined in Figure 1A. Large-area, crack-free silica IOFs were fabricated using a coassembly technique,[15] in which polymeric colloidal spheres were allowed to assemble from the SiO_2 sol-gel precursor solution followed by the removal of the organic colloids by heat treatment, leaving behind a highly uniform porous network (Figure 1B). The entire structure was first functionalized by exposure to vapors of an alkylchlorosilane bearing a functional group, R_1. This R_1 surface functionality was then locally erased and the surface reactivated by exposing the porous inverse opal to oxygen plasma through a removable mask.[16] As a mask, we used slabs of cured poly(dimethyl siloxane) (PDMS) that were sealed to the surface under slight pressure and peeled off after the exposure without damaging the structure. Exposing the selectively oxidized IOF to the vapors of a second alkylchlorosilane bearing a functional group, R_2, now adds a new functionality to surface sites that were not protected by the mask in the previous step. Further plasma-etching through a different mask generates a pattern that is composed of three different surface functionalities (Figure 1A). This process can be repeated many times to produce a surface with a highly diverse, spatially defined chemistry.

Received: June 8, 2011
Published: July 18, 2011

dx.doi.org/10.1021/ja2053013 | *J. Am. Chem. Soc.* 2011, 133, 12430–12432

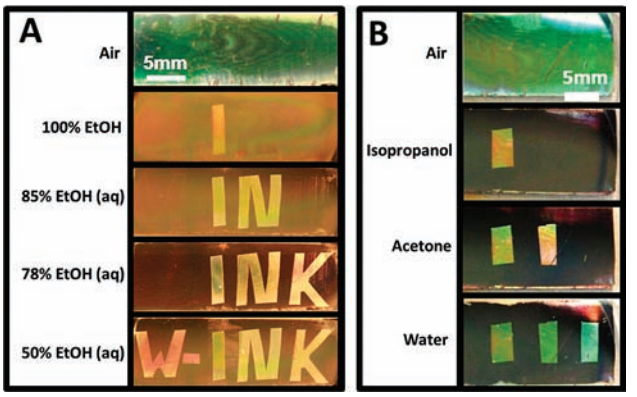

Figure 2. (A) Optical images of an IOF in which the word "W-INK" is encoded via the surface chemistry in an IOF: "W-" 13FS, "I" DEC, "N" 3FS, "K" TMS, background ROH. In different water−ethanol mixtures, different words appear. (B) Optical images of a film encoded with three bars (from left) 13FS, DEC, 3FS, displaying distinct optical patterns when immersed in the common solvents, water, acetone, and isopropanol.

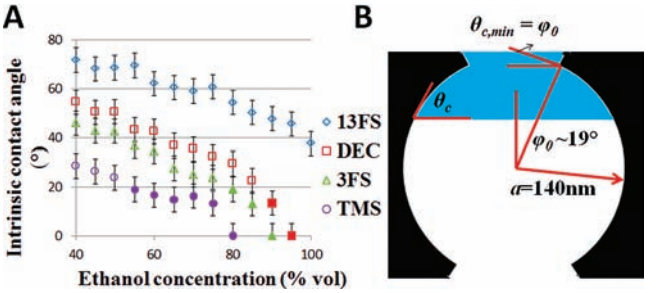

Figure 3. (A) Measured contact angles from different ethanol concentrations in water on flat silicon surfaces after exposure to 13FS, DEC, 3FS, TMS vapors. Filled markers indicate that regions of an IOF functionalized with the same groups are being infiltrated by the corresponding EtOH/water mixture. (B) Schematic of a liquid front propagating through a single unit cell of an inverse opal.

Although it has been previously shown that such masked plasma etching can be used to locally pattern self-assembled monolayers (SAMs) in 2D,[16] the extension of this approach to 3D porous media is less intuitive, and has not been explored. To obtain a high resolution from this type of shadow-patterning process on a 3D porous surface, the modification process should be nearly isotropic to prevent shadowing effects from one pore to the next. In addition, the surface modification front must move sufficiently slowly that its penetration depth can be controlled. Under these conditions we can choose an exposure time that allows modification to occur throughout the depth of the structure, while not spreading too far underneath the mask. For the highly symmetric inverse opals used here, which have a relatively small pore diameter (280 nm) and interpore opening (~90 nm), we found that modification occurs on a time scale of several minutes and the width of the lateral interface is comparable to the film thickness. To characterize the interface of the functionalized regions, an IOF was first derivatized uniformly with (1H,1H,2H,2H-perfluorooctyl)silyl (R = 13FS) groups and then etched through a rectangular mask to reveal hydrophilic polar surfaces (referred to altogether as ROH hereafter for simplicity). We found that the pores of the 13FS-functionalized IOF resisted infiltration by most solvents, including liquid precursors of PDMS. Selective infiltration of PDMS prepolymer into the lyophilic (ROH) regions of the crystal followed by thermal curing allowed us to "freeze" in place and characterize the chemical interface. Using SEM, optical microscopy, and optical spectroscopy, we measured wetting interfaces to have widths of 5−20 μm (see Figure S1 in Supporting Information [SI]), which represents the resolution limit of our technique.

Figure 2A shows encoded messages containing five different local functionalities, the patterning appearing optically invisible when dry but displaying four different messages when submerged in specific fluids. The word, "W-INK", is encoded in a SiO_2 inverse opal with combinations of ROH and four different inner-surface SAMs with decreasing hydrophilicity: trimethylsilyl (TMS), 3,3,3-trifluoropropylsilyl (3FS), n-decylsilyl (DEC), and 13FS. While displaying bright color and no pattern in air, the functionalized 3D photonic crystal reveals four different words when submerged in ethanol (EtOH), 85% (vol) EtOH in water, 78% EtOH, and 50% EtOH, due to the area-specific wetting of the functionalized IOF by liquids with increasing surface tension and the resulting disappearance of the color in the infiltrated regions. In all cases, the message evaporates rapidly upon drying of the sample (see movie in SI for example). The encoding via surface chemistry of many fluid-specific optical responses into a single material that appears homogeneous when dry is a type of multilevel encryption that could find many applications in security or authentication. In this "Watermark-Ink" (W-INK) concept, different "watermarks" are revealed only by a very specific set of fluids.

The induction of fluid-specific optical responses also implies that W-Ink could find use as a colorimetric indicator for liquids on the basis of wettability. As a proof of concept, Figure 2B shows a sample patterned with three stripes (13FS, DEC, 3FS) with an ROH background. Different color patterns are produced when the film is submerged in the three common cleanroom solvents: isopropanol, acetone, and water.

Two notable properties of the above results are (i) that the nonwetting state can be observed even for very low-surface-tension liquids (e.g., γ_{EtOH} = 22.3 mN/m, $\gamma_{PDMS} \approx$ 20 mN/m) and (ii) the high selectivity of wetting occurring for quite similar liquids or their mixtures. To explain these properties, Figure 3 shows measured contact angles for different water−ethanol mixtures on flat silicon wafers functionalized with 13FS, DEC, 3FS, and TMS. This correlates the estimated intrinsic contact angle with the onset of the infiltrated state. Notably, the threshold between the nonwetted and wetted states (e.g., Figure 2) occurs in the contact angle range $\theta \approx 20°$ in all cases. Resistance to wetting down to such a low contact angle can be explained by the reentrant curvature (overhang) associated with the narrow openings between adjacent pores.[17] In an ideal IOF, all pores have the same diameter and spherical geometry and are connected to their nearest neighbors by interpore necks of identical radii. In such a symmetric system, the free-energy landscape associated with the propagation of the liquid front from one pore to the next is the same everywhere throughout the structure. Therefore, the global nonwetting state should occur when there is an energy barrier associated with propagation of the liquid front through a single unit cell. Figure 3B shows a schematic of a fluid front advancing through a single unit cell. For a pore having a radius, R = 140 nm and an opening of 90 nm in diameter at the top, the azimuthal angle subtended by the opening is $\varphi_0 \approx 19°$. The total free-energy change associated

with the liquid front having descended from the top of the pore down to an azimuthal angle, φ, is given by: $\Delta G = \gamma_{la}\pi R^2([(\sin^2 \varphi) - (\sin^2 \varphi_0)] - 2(\cos \theta_c)(\cos \varphi_0 - \cos \varphi))$, where γ_{la} is the liquid−air surface tension and θ_c is the intrinsic contact angle. Since the geometry at the top of the pore is reentrant with respect to the liquid front, there is a trade-off between the energetically favorable liquid−solid interaction (when $\theta_c < 90°$) and the energy cost of the creating liquid−air interface. An energy barrier, and thus a metastable nonwetting state, exists when $(d\Delta G)/(d\varphi)|_{\varphi=\varphi_0} > 0$. This occurs when $\theta_c > \varphi_0$. Therefore, in our geometry, a transition from the nonwetting to the wetting state is expected to occur at $\theta_c = \varphi_0 \approx 19°$, well in the wetting range, and in agreement with what is observed in Figures 2A and 3A.

The remarkable selectivity of wetting observed here can be attributed to the highly regular geometry and defect- and crack-free nature of our IOFs.[15] Unlike typical porous materials, inverse opal photonic crystals fabricated via coassembly[14] have a particularly regular geometry, with uniform pore and pore-neck sizes, that leads to sharply defined wetting thresholds for individual liquids and thus, a high density of localized chemical information. The absence of defects or cracks eliminates the irregular wicking artifacts and enables a high resolution of the wetting patterns.

There are several unique properties of this material platform that lend it to many possible applications: (i) the high selectivity of infiltration, (ii) the range of fluid surface tensions across which this selectivity is observed, and (iii) its coupling to an easily detectable optical response. Beyond encryption we foresee that this system could find use as an optical litmus test for surface tension, as easy to use as pH paper is for detecting pH, but exploiting a property that exists for all liquids (surface tension) and thus could be used to distinguish between similar liquids of any class, as well as a self-reporting biochemical sensor. We anticipate that our straightforward procedure for patterning the surface chemistry throughout 3D porous films could also be generalized to many types of porous media with different pore-sizes and geometries, uncovering a wide variety of other new phenomena and applications.

■ ASSOCIATED CONTENT

Supporting Information. Detailed experimental procedures and interface characterization; movie depicting appearance and disappearance of encrypted messages. This material is available free of charge via the Internet at http://pubs.acs.org.

■ AUTHOR INFORMATION

Corresponding Author
ibburges@fas.harvard.edu; jaiz@seas.harvard.edu

■ ACKNOWLEDGMENT

We thank Dr. W. Noorduin, Dr. T. S. Wong and Dr. P. Kim for enlightening discussions. This work was supported by the Air Force Office of Scientific Research Award # FA9550-09-1-0669-DOD35CAP. I.B.B. acknowledges support from the Natural Sciences and Engineering Research Council of Canada through the PGS-D program. L.M. acknowledges fellowship support from the Department of Homeland Security (DHS) administered by the Oak Ridge Institute for Science and Education (ORISE) through an interagency agreement between the US Department of Energy (DOE) and DHS under DOE Contract DE-AC05-06OR23100. Electron microscopy was performed at Harvard's Center for Nanoscale Systems.

■ REFERENCES

(1) Clelland, C. T.; Risca, V; Bancroft, C. *Nature* **1999**, *399*, 533–534.
(2) Marguiles, D.; Felder, C. E.; Melman, G.; Shanzer, A. *J. Am. Chem. Soc.* **2007**, *129*, 347–354.
(3) Thomas, S. W.; Chiechi, R. C.; Lafratta, C. N.; Webb, M. R.; Lee, A.; Wiley, B. J.; Zakin, M. R.; Walt, D. R.; Whitesides, G. M. *Proc. Natl. Acad. Sci. U.S.A.* **2009**, *106*, 9147–9150.
(4) Albert, K. J.; Lewis, N. S.; Schauer, C. L.; Sotzing, G. A.; Stitzel, S. E.; Vaid, T. P.; Walt, D. R. *Chem. Rev.* **2000**, *100*, 2595–2626.
(5) Lonergan, M. C.; Severin, E. J.; Doleman, B. J.; Beaber, S. A.; Grubbs, R. H.; Lewis, N. S. *Chem. Mater.* **1996**, *8*, 2298–2312.
(6) Bonifacio, L. D.; Puzzo, D. P.; Breslav, S.; Wiley, B. M.; McGreer, A.; Ozin, G. A. *Adv. Mater.* **2010**, *22*, 1351–1354.
(7) Yin, Y. D.; Lu, Y.; Gates, B.; Xia, Y. N. *J. Am. Chem. Soc.* **2001**, *123*, 8718–8729.
(8) Aizenberg, J.; Black, A. J.; Whitesides, G. M. *Nature* **1999**, *398*, 495–498.
(9) Whitesides, G. M.; Grzybowski, B. *Science* **2002**, *295*, 2418–2421.
(10) Smith, R. K.; Lewis, P. A.; Weiss, P. S. *Prog. Surf. Sci.* **2004**, *75*, 1–68.
(11) Weissbuch, I.; Addadi, L.; Lahav, M.; Leiserowitz, L. *Science* **1991**, *253*, 637–645.
(12) Yang, J. P.; Meldrum, F. C.; Fendler, J. H. *J. Phys. Chem.* **1995**, *99*, 5500–5504.
(13) Lee, J.-T.; George, M. C.; Moore, J. S.; Braun, P. V. *J. Am. Chem. Soc.* **2009**, *131*, 11294–11295.
(14) Martinez, A. W.; Phillips, S. T.; Whitesides, G. M. *Proc. Natl. Acad. Sci. U.S.A.* **2008**, *105*, 19606–19611.
(15) Hatton, B. D.; Mishchenko, L.; Davis, S.; Sandhage, K. H.; Aizenberg, J. *Proc. Natl. Acad. Sci. U.S.A.* **2010**, *107*, 10354–10359.
(16) Lin, M.-H.; Chen, C.-F.; Shiu, H.-W.; Chen, C.-H.; Gwo, S. *J. Am. Chem. Soc.* **2009**, *131*, 10984–10991.
(17) Tuteja, A.; Choi, W.; Mabry, J. M.; McKinley, G. H.; Cohen, R. E. *Proc. Natl. Acad. Sci. U.S.A.* **2008**, *105*, 18200–18205.